HLPG-Based Bandwidth-Enhanced Flat-Top Filter and Its Application to OAM Mode Converter

Zhang Meng
Graduate School of the Science and Technology
Shizuoka University
Hamamatsu, Japan
mengzhang1996@163.com

Taiga Suzuki
Graduate School of the Faculty Engineering
Shizuoka University
Hamamatsu, Japan
suzuki.taiga.17a@shizuoka.ac.jp

Hua Zhao
School of the Computer and Electric Information anization
Nanjing Normal University
Nanjing, China
zhaohua@njnu.edu.cn

Chengliang Zhu
College of Information Science and Engineering
Northeastern University
Shenyang, China
zhuchengliang@neuq.edu.cn

Peng Wang
College of the Electronic Engineering
Xiaozhuang University
Nanjing, China
2017025@njxzc.edu.cn

Hongpu Li
Graduate School of the Science and Technology
Shizuoka University
Hamamatsu, Japan
ri.kofu@shizuoka.ac.jp

***Abstract*—A bandwidth-enhanced flat-top OAM mode converter is proposed and demonstrated both theoretically and experimentally, which is realized by using a helical long-period fiber grating but operated at DTP wavelength of the $LP_{1,10}$ mode.**

Keywords—Flat-top band-rejection filter, helical long-period fiber grating, OAM mode converter

I. INTRODUCTION

In the past decades, long period fiber grating (LPG)-based band-rejection filter had been comprehensively studied [1-6]. However, due to some of the unrealistic requirements in fabrication, such as the Sinc-like apodization [2], the precisely inserted phase-shifts [3], and ultra-long length grating (>50 cm) [4] etc., to precisely control the bandwidth and the spectral profile of the LPG-based rejection filter has still been a great challenge to us and has rarely been resolved to date. As an alternative approach, recently the helical long-period fiber grating (HLPG)-based band-rejection filters have been proposed and experimentally demonstrated [7-14]. Owing to the unique characteristics, e.g., the orbital angular momentum (OAM)-like eigenmodes, the spin-dependent mode selection rules, and the inherent compatibility with the other fiber devices, the HLPGs have recently attracted great research interest and have been found versatile applications besides the band-rejection filters [15-20].

Upon to the HLPG-based band-rejection filter, two critical parameters, i.e., the flat-top bandwidth and the rejection depth, are generally used to evaluate its performances. However, to be the same as the LPGs, it is rather difficult to obtain HLPG with a broadband and a flat-top spectrum, simultaneously. To date, mainly three kinds of the HLPG-based devices have been proposed and demonstrated. The first one is based on utilization of two cascaded HLPGs proposed by Shin et al. [7], where a rejection filter with a tunable bandwidth of several tens nanometer had been demonstrated. However, the fluctuation in rejection depth presented there was so large (>10 dB) that the flat-top performance cannot be obtained. As an alternative, the group of ours have proposed and demonstrated another HLPG-based band-rejection filter, where two consecutively cascaded HLPGs but with different helicities were proposed and utilized. As a result, a flat-top band-rejection filter with a rejection depth of ~17 dB and a bandwidth of ~14 nm@-16dB had been obtained [8, 9]. However, in order to obtain an ideal flat-top spectrum, both the rejection depths and the resonant wavelengths of the two cascaded HLPGs must be precisely matched during their fabrication, which considerably increases the fabrication difficulties. More importantly, the obtained filter is of polarization-dependence, which inevitably restrains the filter from the practical applications. The second approach is the one based on the use of a phase-modulated HLPG, which was originally proposed and demonstrated by our group [10]. As a result, a polarization-independent filter with a bandwidth of ~10 nm@-20dB has been successfully achieved. However, the obtained bandwidth is still narrow, not wide enough to cover the whole C or the L band in fiber communication system. Moreover, due to the additional phase-modulation applied to the HLPG, the grating pitch is no longer a constant, i.e., the local pitches change as a function of the positions, how to precisely control the local pitches for the optimized HLPG then becomes a great challenge. The third approach is the one proposed and numerically demonstrated by Ren et al. [11], where they exploited a linearly-chirped and the length- apodized HLPG but operating at the dispersion-turning point (DTP). The rejection filter with a flat-top broad bandwidth of ~100 nm and the rejection depth larger than 30 dB have been numerically demonstrated, however no experimental results have been provided. Recently, by exploiting the DTP method to two-mode fiber (TMF) and single-mode fiber (SMF), respectively, Zhao et al. [12] and Zhou et al. [13] have experimentally demonstrated the HLPG-based wide-band OAM mode-converter, respectively, where a rejection filter with a bandwidth of ~200 nm @-10dB has been successfully demonstrated. However, all the filters mentioned above are not the flat-top ones. Most recently, by using the aforementioned phase-modulation method combined with the DTP method, Zhu et al have numerically demonstrated an ultra-broadband OAM mode generator with a bandwidth of ~ 469 nm and a conversion efficiency of ~100% [14]. However, the required length for the designed HLPG is too longer to be practically realized and no experimental results can be provided.

In this study, we have proposed and experimentally demonstrated a bandwidth-enhanced flat-top filter, which is based on a HLPG but operated precisely at DTP of the mode $LP_{1,10}$. Unlike the most of the HLPG-based OAM generators reported to date where both the flat-top and broad band second-order OAM mode centered at a wavelength of ~1520 nm have rarely been realized simultaneously, here a first-order OAM mode generator with a flat-top bandwidth of ~48 nm@-

10dB, and a conversion efficiency larger than 90% has been successfully demonstrated.

II. Principle of the Bandwidth-Enhanced HLPG and the Simulation Results

It is commonly known that, in long-period fiber gratings (LPGs) as well as the HLPGs, the mode couplings generally occur between the core mode and the distinct cladding modes. In order to obtain non-zero coupling coefficient, the following equation should be satisfied [19]

$$\beta_p - \beta_q - 2\pi \cdot m \cdot 2\pi / \Lambda = 0 , \quad (1)$$

where β_p (=$2\pi n_p/\lambda$) and β_q (=$2\pi n_q/\lambda$) are the propagation constants of these two modes, n_p and n_q are the effective indices of these two modes, λ denotes the resonant wavelength of the HLPG. This equation corresponds to the phase-matching condition for resonant coupling between the mode p and q under the perturbation of the m^{th} diffraction of a HLPG, namely the m^{th} order of the HLPG. On the other hand, since the mode couplings occur between the core mode and the distinct cladding modes, the modal dispersion and its effects cannot be neglected, which could strongly affect the spectral performances of the grating, especially to the bandwidth of the rejection filter (notch). For all cases considering the mode dispersion effect, the rejection bandwidth for a HLPG can be deduced from Eq. (1) and approximately expressed as [20, 21]

$$\Delta\lambda_B \approx \frac{\Delta\lambda_0}{\left|1 - \Lambda(\lambda)\cdot\left(d\Delta n_{eff}/d\lambda\right)\right|} = \frac{\Delta\lambda_0}{\Delta n_{eff}\cdot\left(\left|d\Lambda/d\lambda\right|\right)}, \quad (2)$$

where $\Delta\lambda_B$ and $\Delta\lambda_0$ represent the notch bandwidth with and without considering mode dispersion effect, respectively. λ represents the wavelength. Δn_{eff} represents the effective index difference between the core and the coupled cladding mode. $\Lambda(\lambda)$ represents the HLPG's pitch. Under the assumptions that the considered HLPG is rather strong with rejection depth larger than 20 dB ($\kappa L \approx \pi/2$) and the power of the core mode is fully coupled into one particular cladding mode, the 20 dB bandwidth of the local resonance peak $\Delta\lambda_B$ can be obtained as [21]

$$\Delta\lambda_B \approx 0.06\kappa \frac{\Lambda_0^{\,2}}{\left|d\Lambda/d\lambda\right|}, \quad (3)$$

where κ represents the coupling coefficient between the mode LP_{01} and the coupled higher-order mode. From the Eq. (3), it is easy to find that bandwidth $\Delta\lambda_B$ is inversely proportional to $|d\Lambda/d\lambda|$. In other word, the broadest dip can be expected to achieve if the HLPG is operated at a nominal wavelength λ_0, namely the DTP wavelength, where the condition $d\Lambda/d\lambda$=0 is satisfied. In such case, bandwidth $\Delta\lambda_B$ can no longer be determined by Eq. (2), instead, it can be determined by [22]

$$\Delta\lambda_B \approx \Lambda_0 \left\{ \frac{0.06\kappa}{\left|d^2\Lambda/d\lambda^2\right|_{\lambda=\lambda_0}} \right\}^{1/2} . \quad (4)$$

The Eq. (3) obviously indicates that, for a LPG as well as the HLPG, the bandwidth $\Delta\lambda_B$ is inversely proportional to the magnitude of $d\Lambda/d\lambda$. Therefore, it is easy for one to come across the conclusion that if the HLPG is arranged to operate at or very close to the DTP wavelength, the obtained rejection dip would be of the flat-top and the broad one, in other word, the broad and the flat-top bandwidth $\Delta\lambda_B$ can be expected to obtain
simultaneously.

In order to validate the above presumption, we optimally designed the HLPGs, which are assumed to be fabricated in conventional single-mode fiber. All the parameters, such as the diameters of the core and the cladding are assumed to be 125 μm and 8.2 μm, respectively. The refractive indices of the core, the cladding, and the surrounding material are assumed to be, 1.458, 1.4532, and 1.0, respectively. Moreover, the wavelengths ranging from 1400 nm to 1700 nm are particularly considered in this study. By numerically solving the dispersion equations described in [23], we obtained the pitch spectra for different cladding modes, which are shown in Fig. 1(a), where the curves $LP_{1,8}$, $LP_{1,9}$, …, and $LP_{1,12}$ represents the cases that the resonant couplings occur between the mode LP_{01} and the modes $LP_{1,8}$ -$LP_{1,12}$, respectively. It can be seen that within the S-L bands of the fiber communication, i.e., the wavelengths ranging from 1500 nm to 1600 nm, there exists a DTP only for the mode of $LP_{1,10}$. For the sake of precisely showing the DTP pitch, the curve $LP_{1,10}$ shown in Fig. 1(a) is enlarged and individually depicted in Fig. 1(b). From the Fig. 1(b), it can be seen that at point of (1560 nm, 222.32 μm), the magnitude of $d\Lambda/d\lambda$ is precisely equal to zero.

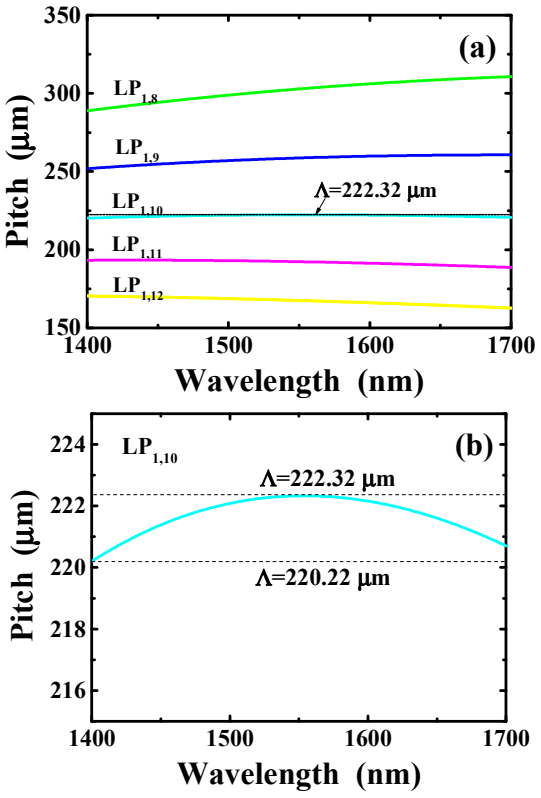

Fig. 1. (a) The dispersion spectra of the pitch for modes $LP_{1,8}$-$LP_{1,12}$. (b) The dispersion spectrum for mode $LP_{1,10}$.

Next, the HLPG with a rejection depth larger than 10 dB was considered in the simulations, which was particularly

designed to have a pitch right as 222.32 μm and the other three pitches, respectively. In accordance, the mode coupling occurring between the LP_{01} and $LP_{1,10}$ at a wavelength ranging from 1400 to 1700 nm is considered in this study. Transmission spectra of the HLPGs were calculated by using the transfer matrix method [24]. The calculated spectra are shown in Fig. 2, where the index-modulation is adopted as 1.92×10^{-4}. Length of the HLPGs is assumed to be 4.0 cm (with 180 periods). From the Fig. 2(a) , it is seen that while the grating's pitch is assumed to be 222.32 μm, a band-rejection filter with a flat-top bandwidth of ~49 nm@-10dB at a central wavelength of 1560 nm has been successfully obtained, which agree perfectly with what we deduce from the Eq. (2) and the DTP positions shown in Fig. 1(b). However, from the Fig. 2(b) where four different pitches, i.e., the ones with a deviation of 0, 0.1, 0.2, and 0.3 μm to the DTP pitch of 222.32 μm, are particularly adopted, it can be found that even a small deviation in DTP pitch, like 0.2 μm away from the 222.32 μm, it will result in a considerable change in the rejection spectrum and make the dual peaks appeared instead of the flat-top band. The above results implicitly mean that by using the DTP method, although the bandwidth-enhanced flat-top can be expected to be obtained, the pitch must be precisely controlled with resolution of the sub-micrometer, which would be a great challenge to precisely control such fine pitch in practical fabrication.

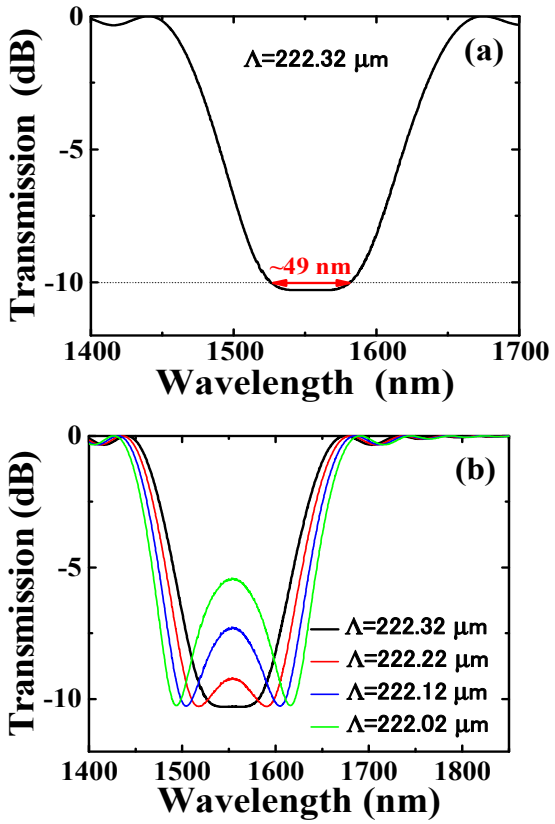

Fig. 2. Simulation results for transmission spectra the HLPGs where the maximum index-modulation is assumed to be $1.64\text{x}10^{-4}$, and the pitches are assumed to be (a) 222.32 μm and (b) the ones with a deviation of 0, -0.1, -0.2, and -0.3 μm in DTP pitch.

III. FABRICATION OF THE DESIGNED HLPG AND THE EXPERIMENTAL RESULTS

To experimentally verify the above proposal, the designed HLPG was fabricated by using the SMF. The grating pitch was especially adopted as 667 μm, which is exactly three-time of the pitch required for the first-order HLPG. The fabrication setup is shown in Fig. 4, which is nearly the same as what we had used in [25]. Unlike the other CO_2 laser direct-writing techniques where in general the fiber is directly heated by the laser beam through a focused lens, here a sapphire tube is specially designed and utilized in place of the focused lens, as a result, the fiber within the tube region can be homogeneously heated and twisted. More importantly, pitch of the HLPG can be precisely controlled by adjusting the moving speed of the fiber-loaded stage and the rotator speed, accuracy of the pitch obtained in our setup is estimated to be ±0.5 μm, which is mainly determined by position precision of the utilized translation-stage. In order to make the fabricated third-order HLPG strong enough, 90 periods of the HLPG was adopted.

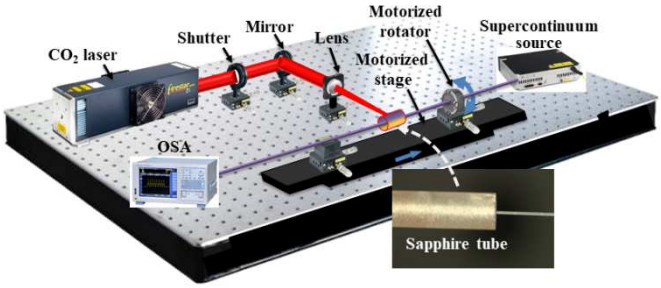

Fig. 3. Experimental setup for fabrication of the proposed third-order HLPG.

Figure 4 shows the measurement result for transmission spectrum of one fabricated HLPG. From this figure, it is found that a flat-top band-rejection filter with a depth of ~10 dB and a bandwidth of ~48 nm@-10 dB has been successfully obtained, which is located at a central wavelength of ~1553.0 nm. Compared with the results shown in Fig. 3(b), especially the result of the case Λ=222.12, it can be seen that although the obtained bandwidth and rejection-depth have a little different from the simulation ones, which may arise from the pitch deviation produced during the fabrication, the experimental results agree well the simulation ones, which in return indicates that the proposed band-enhanced method by using the third-order HLPG really works.

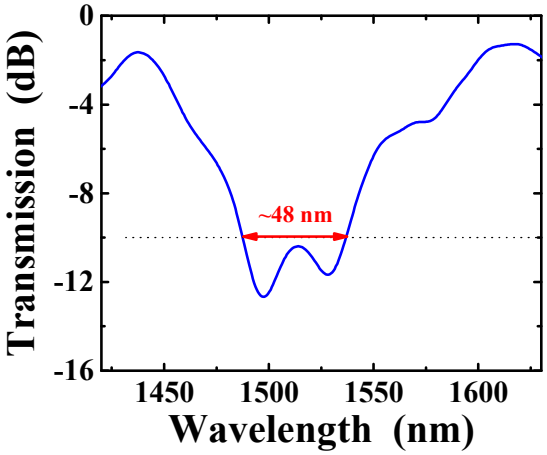

Fig. 4. The measuring result for transmission spectrum of the fabricated HLPG.

IV. Measurement Results for OAM Mode Originated from the Fabricated HLPG

It has already been established both theoretically and experimentally that HLPG can be used as all-fiber OAM mode converter [17, 19]. In the following, we experimentally demonstrate that the proposed and fabricated HLPG could also be used as a broadband flat-top OAM mode converter. The experimental setup for measuring the OAM modes is shown in Fig.5, where a tunable laser with a turning ranging from 1480 to 1600 nm and resolution of 1 pm in wavelength is used as the light source. The light from the tunable laser is split into two arms by a 3 dB coupler, as is shown in Fig. 5. One beam is directed into the testing object, i.e., the fabricated HLPG and then collimated through the beam splitter (BS) by using an objective lens (10x/40x) right at end of the same HLPG. The other light beam is used as the spherically reference one in order to produce the spiral-like interference pattern with the first beam at the imaging plane of the CCD (IR camera: Hamamatsu Photonics C2741-03). A polarization controller (PC) and an attenuator are employed to adjust the visibility of the resulted interference fringes. The fabricated HLPG whose spectrum is shown in Fig. 4 was used as the testing object. The measurement results are shown in Fig. 6, where the insets (a) and (b) represents the intensity and phase distributions of the OAM mode operating at the wavelength of 1497.0 nm, whereas the insets (c) and (d), the insets (e) and (f) represent the intensity and phase distributions of the OAM mode operating at the wavelengths of 1513.0 nm and 1529.0 nm, respectively. For comparison, the spectrum shown in Fig. 4 is also depicted together in Fig. 6. Moreover, three wavelengths (i.e., 1497.0, 1513.0 nm and 1529.0 nm) located at left edge, middle, and right edge of the obtained flat-top band are particularly selected to demonstrate the generation of the first-order OAM modes. Here it must be pointed that intensity distributions shown in this insets (a), (c) and (e) figures are obtained while the reference beam is blocked and

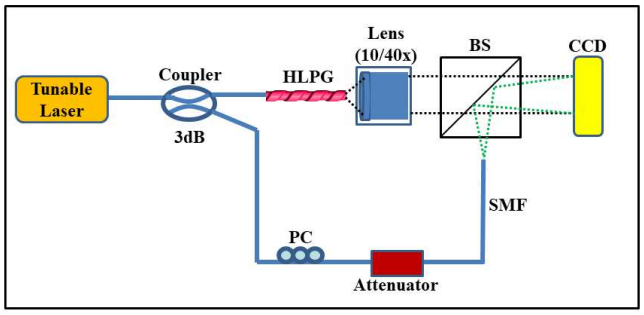

Fig. 5. Experimental setup for testing the OAM mode characteristics of the fabricated HLPG.

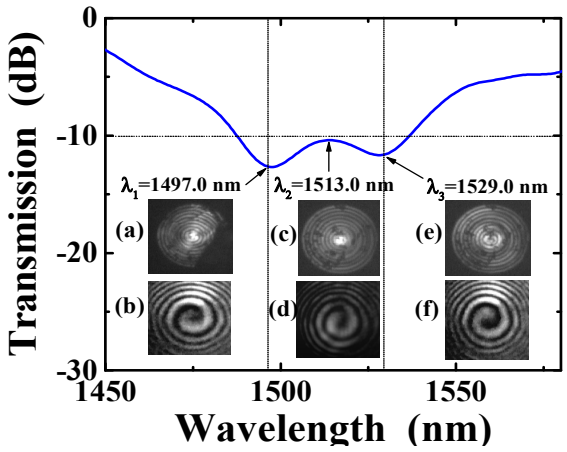

Fig. 6. The intensity and phase distributions of the OAM modes operating at the wavelengths of 1497.0, 1513.0, and 1529.0 nm, respectively. For comparison, the spectrum shown in Fig. 4 is depicted together.

the 40x lens is replaced by a 10x one, so that the whole cross-section of the fiber cladding can be imaged. From Fig. 6, it can be seen that the OAM modes at the selected two wavelengths have been successfully generated and all of them have a conversion efficiency of 90% (10dB in rejection depth). Moreover, from the insets (a)-(e) shown in Fig. 6, it can be seen that the OAM modes obtained at such three typical wavelengths all belong to the same group of the scalar mode LP1,10, which in return means that as expected from the numerical calculation, the mode couplings really happen between the modes LP_{01} and $LP_{1,10}$.

V. Conclusion

A flat-top band-rejection filter has been proposed and demonstrated both theoretically and experimentally, which is realized by using a bandwidth-enhanced flat-top HLPG. As an important application example of the proposed HLPG, a first-order OAM mode with a flat-top bandwidth ~48 nm@-10dB and a conversion efficiency larger than ~90% has been successfully demonstrated, which manifests that the proposed HLPG may find the potential applications to broadband OAM mode converter as well as the OAM sensors.

Acknowledgment

This work is partly supported by Yazaki Memorial Foundation for Science & Technology and JSPS KAKENHI Grant (JP 22H01546

References

[1] A. Vengsarkar, P. Lemaire, J. Judkins, V. Bhatia, T. Erdogan, and J. Sipe, "Long-period fiber gratings as band-rejection filters," *J. Lightwave Technol.*, vol. 3, no. 1, pp. 58-65, Jun. 1996.

[2] J. K. Brenne and J. Skaar, "Design of grating-assisted codirectional couplers with discrete inverse-scattering algorithms," *J. Lightwave Technol.*, vol. 21, no. 1, pp. 254-262, May 2003.

[3] L. Chen, "Design of flat-top bandpass filter based on symmetric multiple phase-shifted long-period fiber gratings," *Opt. Commun.*, vol. 205, no. 4-6, pp. 271-276, May 2002.

[4] J. Zhang, P. Shum, S. Li, N. Ngo, X. Cheng, and J. Ng, "Design and fabrication of flat-band long-period grating," *IEEE Photon. Techn. Lett.,* vol. 15, no. 11, pp. 1558-1560, Oct. 2003.

[5] H. Kim, J. Bae, and J. Chun, "Synthesis of flat-top bandpass filters using two-band rejection long-period fiber gratings," *IEEE Photon. Techn. Lett.*, vol. 19, no. 19, pp. 1466-1468, Sep. 2007.

[6] G. Chern and L. Wang, "Design of binary long-period fiber grating filters by the inverse-scattering method with genetic algorithm optimization," *J. Opt. Soc. Am. A*, vol. 19, no. 7, pp. 772-780, Apr. 2002.

[7] W. Shin, B. Yu, Y. Noh, Z. Lee, K. Ko, and K. Oh "Bandwidth-tunable band-rejection filter based on helicoidal fiber grating pair grating of opposite helicities," *Opt. Lett.*, vol. 32, no. 10, pp. 1214-1216, May 2007.

[8] G. Inoue, P. Wang, and H. Li, "Flat-top band-rejection filter based on two successively-cascaded helical fiber gratings," *Opt. Express,* vol. 24, no. 5, pp. 5442-5447, Mar. 2016.

[9] C. Zhu, H. Zhao, P. Wang, R. Subramanian, and H. Li, "Enhanced flat-top band-rejection filter based on reflective helical long-period fiber gratings," *IEEE Photon. Technol. Lett.*, vol. 29, no. 12, pp. 964-966, May 2017.

[10] P. Wang, H. Zhao, and T. Yamakawa, and H. Li, "Polarization-independent flat-top band-rejection filter based on the phase-modulated HLPG," *IEEE Photon. Technol. Lett.*, vol. 32, no. 3, pp. 170-174, Feb. 2020.

[11] K. Ren, M. Cheng, L. Ren, Y. Jiang, D. Han, Y. Wang, J. Dong, J. Liu, L. Yang, and Z. Xi, "Ultra-broadband conversion of OAM mode near the dispersion turning point in helical fiber gratings," *OSA Continuum*, vol. 3, no.1, pp. 77-87, Jan. 2020.

[12] X. Zhao, Y. Liu, Z. Liu, and C. Mou, "All-fiber bandwidth tunable ultra-broadband mode converters based on long-period fiber gratings and helical long-period gratings," *Opt. Express*, vol. 28, no. 8, pp. 11990-12000, Apr. 2020.

[13] M. Zhou, Z. Zhang, L. Shao, S. Liu, Y. Liu, Y. Pang, Z. Bai, C. Fu, W. Cui, L. Qi, and Y. Wang, "Broadband tunable orbital angular momentum mode converter based on a conventional single-mode all-fiber configuration," *Opt. Express*, vol. 29, no. 10, pp. 15595-15603, May 2021.

[14] C. Zhu, L. Wang, Z. Bing, R. Tong, M. Chen, S. Hu, Y. Zhao, and H. Li, "Ultra-broadband OAM mode generator based on a phase-modulated helical grating working at a high radial-order of cladding mode," *IEEE J. Quantum Electron.*, vol. 57, no. 4, 6800307, Aug. 2021.

[15] V. I. Kopp, V. M. Churikov, J. Singer, N. Chao, D. Neugroschl, and A. Z. Genack, "Chiral fiber gratings," *Science*, vol. 305, no. 5680, pp. 74-75, Jul. 2004.

[16] G. Wong, M. Kang, H. Lee, F. Biancalana, C. Conti, T. Weiss, and P. Russell, "Excitation of orbital angular momentum resonances in helically twisted photonic crystal fiber," *Science*, vol. 337, no. 6093, pp. 446-449, Jul. 2012.

[17] C. Alexeyev and M. Yavorsky, "Generation and conversion of optical vortices in long-period helical core optical fibers," *Phy. Rev. A.*, vol. 78, No. 4, 043828, Apr. 2008.

[18] L. Xian, P. Wang, and H. Li, "Power-interrogated and simultaneous measurement of temperature and torsion using paired helical long-period fiber gratings with opposite helicities," *Opt. Express*, vol. 22, no. 17, pp. 20260-20267, May 2014.

[19] H. Zhao, P. Wang, T. Yamakawa, and H. Li, "All-fiber second-order orbital angular momentum generator based on a single-helix helical fiber grating," *Opt. Lett.*, vol. 44, No. 21, pp. 5370-5373, Nov. 2019.

[20] H. Zhao, M. Zhang, and H. Li, "Modal-dispersion effects on the spectra of the helical long-period fibre grating-based components," *Optics Commun.*, vol. 457, pp. 124708, Feb. 2020.

[21] S. Ramachandran, Z. Wang, and M. Yan, "Bandwidth control of long-period grating-based mode converters in few-mode fibers," *Opt. Lett.*, vol. 27, no. 9, pp. 698-700, May 2002.

[22] V. Danhui, M. J. F. Digonnet, and G. S. Kino, "Ultrabroadband single-mode long-period fiber gratings using high-order cladding modes," *J. Appl. Phy.*, vol. 96, no. 11, pp. 5987-5991, Dec. 2004.

[23] T. Erdogan, "Cladding-mode resonances in short- and long-period fiber gratings filters," *J. Opt. Soc. Am. A*, vol. 14, no. 8, pp. 1760-1773 (1997).

[24] T. Erdogan, "Fiber Grating Spectra," *J. Lightwave Technol.*, vol. 15, no. 8, pp. 1277-1294, Aug. 1997.

[25] Peng Wang and H. Li, "Helical long-period grating formed in a thinned fiber and its application to refractometric sensor," *Appl. Opt.*, vol. 55, no. 6, pp. 1430-1434, Feb. 2016.